



IUScholarWorks at Indiana University South Bend

# **The Electrical Properties of the Anterior Stomach of the Larval Mosquito (*Aedes Aegypti*)**

Clark, T. M., Koch, A., & Moffett, D. F.

To cite this article: Clark, T. M., Koch, A., & Moffett, D. F. (2000). "The Electrical Properties of the Anterior Stomach of the Larval Mosquito (*Aedes aegypti*)" *The Journal of Experimental Biology*, 203(Pt 6), 1093–1101.

This document has been made available through IUScholarWorks repository, a service of the Indiana University Libraries. Copyrights on documents in IUScholarWorks are held by their respective rights holder(s). Contact [iusw@indiana.edu](mailto:iusw@indiana.edu) for more information.

## THE ELECTRICAL PROPERTIES OF THE ANTERIOR STOMACH OF THE LARVAL MOSQUITO (*Aedes aegypti*)

THOMAS M. CLARK<sup>1</sup>, ALAN KOCH<sup>2,\*</sup> AND DAVID F. MOFFETT<sup>2</sup>

<sup>1</sup>*Department of Biological Sciences, Indiana University at South Bend, South Bend, IN 46634-7111, USA and*

<sup>2</sup>*School of Biological Sciences, Washington State University, Pullman, WA 99164-4236, USA*

\*e-mail: kocha@wsu.edu

*Accepted 17 January; published on WWW 21 February 2000*

### Summary

The electrical properties of the anterior stomach of the larval mosquito (*Aedes aegypti*) were determined. At late times after cannulation, the intraluminal space constant was 936  $\mu\text{m}$ , which is almost as long as the isolated tissue itself. At this time, the resistance of the apical cell membranes dominates the transcellular resistance; it is approximately 14 times the resistance of the basal cell membrane. Two physiologically distinct epithelial cell types were identified. One type has a stable basal potential of approximately 65 mV and responds to 5-

hydroxytryptamine with hyperpolarization. The second cell type initially shows a basal potential of 100 mV. However, this basal potential decays in the first few minutes in parallel with the decay of the transintestinal potential. This latter cell type does not respond to 5-hydroxytryptamine.

Key words: mosquito, *Aedes aegypti*, midgut, larva, intracellular potential, 5-hydroxytryptamine.

### Introduction

The ion-transport properties of the insect midgut are critically important for maintaining the appropriate ionic concentrations and pH for digestion and absorption. The pH of the midgut also plays an important role in determining susceptibility to biological control agents such as *Bacillus thuringiensis* (Knowles, 1994). Despite the importance of this system, most of our information about insect midgut ion transport is from studies on the apparently unique midgut of lepidopteran larvae (for reviews, see Dow, 1986; Clements, 1992).

The anterior stomach region of the larval mosquito is known to be an alkalinizing organ and apparently regulates the alkalinizing process *via* a neural or hormonal mechanism (Dadd, 1975, 1976). Recently, cDNA clones of two V-ATPase subunits have been isolated from the midgut of *Aedes aegypti* larvae (Gill et al., 1998), and a high level of expression of one of these subunits was observed in anterior midgut (Filippova et al., 1998). However, the relationship between the expression of V-ATPase and transepithelial ion transport is unclear.

In an initial study of the ion-transport properties of the larval mosquito midgut, Clark et al. (1999) established that the anterior stomach of *Aedes aegypti* generates a lumen-negative transepithelial potential that is relatively large in magnitude (approximately 60 mV) immediately after dissection, but which rapidly decays to  $-10\text{ mV}$  or less. At this time, the biogenic amine 5-hydroxytryptamine hyperpolarized the tissue to a value approximately 50% of its initial value when applied at concentrations previously reported to be present in

hemolymph (Clark and Bradley, 1997; Clark et al., 1999). This lumen-negative potential stands in marked contrast to the lumen-positive potential across the larval lepidopteran midgut (Klein et al., 1996) and appears to be driven by different primary motive forces. Other mechanisms, such as those responsible for the apparently homologous ability to generate extremely alkaline conditions, seem to be shared between the two groups (Clark, 1999).

### Materials and methods

#### *Mosquitoes*

*Aedes aegypti* (Vero Beach strain) eggs were provided by Dr Marc Klowden, University of Idaho, USA, from a continuously maintained colony. Eggs were hatched in deionized water, and larvae were maintained in deionized water at 26 °C on a 16 h:8 h L:D photoperiod. The water was replaced each morning, and the larvae were fed at that time with ground Tetramin flakes (Tetrawerke, Melle, Germany).

#### *Solutions and chemicals*

The saline used in all experiments was based on the description by Edwards (1982a,b) of larval *Aedes* hemolymph composition and consisted of the following (in  $\text{mmol l}^{-1}$ ): NaCl, 42.5; KCl, 3.0; MgSO<sub>4</sub>, 0.6; CaCl<sub>2</sub>, 5.0; NaHCO<sub>3</sub>, 5.0; succinic acid, 5.0, malic acid, 5.0; L-proline, 5.0; L-glutamine, 9.1; L-histidine, 8.7; L-arginine, 3.3; dextrose, 10.0; Hepes, 25. pH was adjusted to 7.0 with NaOH.

*Perfusion pipettes*

Perfusion pipettes were made from glass capillary pipettes (100  $\mu\text{l}$ , VWR). An initial pull on a David Kopf Instruments vertical pipette puller (model 700B) was followed by hand-forging to form a pipette with a bulbous tip approximately 200  $\mu\text{m}$  in diameter and 400  $\mu\text{m}$  in length that could be inserted into the gut lumen and tied in place using a fine human hair.

*Perfusion of gut sections*

A Harvard Apparatus multi-speed transmission infusion/withdrawal perfusion pump (model 902) was modified for simultaneous infusion and withdrawal, allowing perfusion of the gut section with a negligible distending pressure gradient across the epithelium. Micromanipulators (Brinkmann) were used to hold and manipulate the infusion and withdrawal pipettes. Sections of the anterior stomach were isolated in a 1 ml bath. The withdrawal-side pipette was then inserted into the lumen and tied in place. The infusion-side pipette was inserted into the other end of the gut section and also tied. Gut sections that showed a sudden drop in transepithelial potential (TEP) as the perfusion/voltage-sensing pipette was tied, and those with obvious leaks, were rejected. The perfusion pump and bath flow were then started. The bath was perfused by gravity at a rate of approximately 15  $\text{ml h}^{-1}$  with oxygen-saturated saline (100%  $\text{O}_2$ ), while the lumen of the isolated gut section was perfused from anterior to posterior with identical but non-oxygenated saline at a rate of 62.3  $\mu\text{l h}^{-1}$ .

*Electrophysiological measurements*

A Ag/AgCl electrode was inserted into the perfusion pipette to within 5 mm of the tip. In later experiments, a second Ag/AgCl electrode was inserted into the outflow pipette. Conventional microelectrodes were pulled from Omega dot filament glass (1.5 mm o.d., 0.75 mm i.d.; Frederick Haer), filled with 500  $\text{mmol l}^{-1}$  KCl and connected to Ag/AgCl electrodes. Tip resistances were not determined. The reference potential for these measurements was the bathing solution, which was connected *via* a KCl/agar bridge to a Ag/AgCl electrode.

In early experiments, voltage deflection after current injection at the input pipette was compared with that at the microelectrode. In later experiments, the voltage deflection at the outflow pipette was also measured.

Current was injected briefly through the perfusion-side electrode, and voltage deflections were recorded at the injection pipette and in an intracellular or intraluminal microelectrode. In later experiments, the voltage deflection at the outflow pipette was also recorded. The direction of current flow was then reversed and the injection repeated.

*Application of 5-hydroxytryptamine*

In some experiments, after successful luminal or intracellular positioning of the microelectrode and initial measurements, bath flow was stopped, and 5-hydroxytryptamine (5-HT) added to the bath and mixed to a final concentration of  $10^{-4}$   $\text{mmol l}^{-1}$ .

*Data acquisition and statistical analyses*

Data were acquired through high-impedance amplifiers using data acquisition software (Sable Systems, Las Vegas, NV, USA). Data were sampled at 0.11 s intervals, with each sample an average of 112 readings. Results are reported as means  $\pm$  S.E.M. followed by the number of experiments in parentheses. Mean values were compared using a two-sided Student's *t*-test. All times are measured from the time the gut was cannulated.

**Theory**

Measurement of the electrical parameters of a tubular organ using cable properties has been discussed previously including in the work of Boupaep and Sakin (1979), Leyssens et al. (1992) and, of course, Hodgkin and Rushton (1946). We shall go over it briefly here.

The possible pathways of current flow in the gut in these experiments as well as the symbols used are shown in Fig. 1A. Longitudinal current enters the lumen and either proceeds along the lumen or crosses the tubular wall to the outside solution. By the downstream end, all the current must have crossed the walls. Since the tubular walls are made up of cells with tight junctions, some of the radial current may conceivably travel longitudinally from cell to cell. Most of the radial current, however, may be expected to pass through the basal cell membrane to the outside bathing solution. The equations for this system are:

$$V(x) = K_1 \exp(-\alpha x) + K_2 \exp(\alpha x) + K_3 \exp(-\beta x) + K_4 \exp(\beta x), \quad (1)$$

$$\Phi(x) = K_5 \exp(-\alpha x) + K_6 \exp(\alpha x) + K_7 \exp(-\beta x) + K_8 \exp(\beta x), \quad (2)$$

where  $\alpha^2 + \beta^2 = (2\rho_1/ar_a) + \{[2\rho_2/b(2a+b)]\} \{(a/r_a) + [(a+b)/r_b]\}$  and  $\alpha^2\beta^2 = 4\rho_1\rho_2(a+b)/ab(2a+b)r_ar_b$ ,  $V(x)$  is the change in luminal voltage upon injection of a total current  $M$ ,  $\Phi(x)$  is the change in cellular voltage,  $r_a$  is the apical membrane resistance and  $r_b$  is the basal membrane resistance, both in  $\Omega \text{ cm}^2$ . The length of the tube is  $W$  (cm). The internal radius of the tube is  $a$  and the height of the cells is  $b$  (both in cm). The resistivity of the luminal solution is  $\rho_1$  ( $\Omega \text{ cm}$ ), and the effective resistivity in the cells is  $\rho_2$  ( $\Omega \text{ cm}$ ). The longitudinal current densities are  $I(x)$  in the lumen and  $i(x)$  in the cells (both in  $\text{A cm}^{-2}$ ). The radial current densities are  $J(x)$  across the apical membrane and  $j(x)$  across the basal membrane (both in  $\text{A cm}^{-2}$ ). A paracellular resistance,  $r_p$ , is in parallel with the series combination of  $r_a$  and  $r_b$ . The effect of cell-to-cell coupling is incorporated into  $\rho_2$ . Thus, if the entire lateral cell surface allows current to flow from cell to cell,  $\rho_2$  would take the value of resistivity of the cell fluid; if there is no longitudinal current flow from one cell to another,  $\rho_2$  is infinite (see Fig. 1). The values of the constants  $K_1$ – $K_8$  are determined by the boundary conditions.

If there is no longitudinal flow of current between cells, the system collapses into a simpler one wherein the entire gut wall can be characterized by a single resistance,  $r_m$ , and there is only a single conductivity,  $\rho$ , as depicted in Fig. 1B. The value of

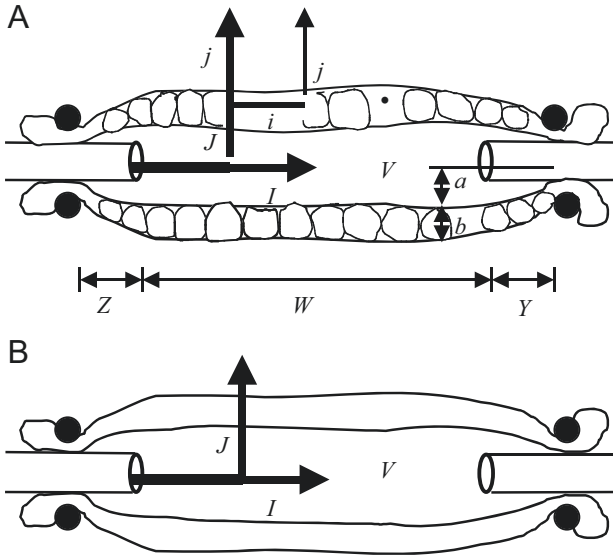


Fig. 1. Diagram of the perfusion system. The symbols used in equations 1–6 are also illustrated.  $a$ , internal radius of the lumen;  $b$ , height of the cells;  $i$ ,  $I$ , longitudinal current density across the apical membranes and in lumen, respectively;  $j$ ,  $J$ , radial current density across the apical and basal membranes, respectively;  $V$ , luminal voltage;  $W$ , length of the tube;  $Y$ ,  $Z$ , end regions of the tube beyond the perfusion pipettes;  $\Phi$ , cellular voltage. (A) Possible pathways of current flow; (B) simplified system in which there is no longitudinal flow of current between the cells.

$r_m$  is given by the series combination of  $r_a$  and  $r_b$  in parallel with the paracellular resistance. The solution for the axial voltage then becomes:

$$V(x) = \frac{M\lambda\rho}{\pi a^2} \frac{\cosh\{(W/\lambda)[1 - (x/W)]\}}{\sinh(W/\lambda)}, \quad (3)$$

where  $\lambda^2 = ar_m/2\rho$ . The combined wall resistance,  $r_m$ , is related to the individual resistances by:

$$r_m = \frac{r_a + [a/(a+b)]r_b}{1 + \{r_a + [a/(a+b)]r_b\}/r_b}. \quad (4)$$

This complicated form to add the membrane resistances is necessary since cell height ( $b$ ) is appreciable compared with luminal diameter ( $a$ ).  $\lambda$  is the space constant of the tissue. This is the standard solution for a terminated leaky tube. If there is no paracellular current flow ( $r_p = \infty$ ),  $r_m$  becomes:

$$r_m = r_a + [a/(a+b)]r_b, \quad (5)$$

which is simply the series sum of the basal and apical resistances.

The total current delivered at the input pipette was known, but some of this current flowed back behind the pipette tip and crossed the epithelium at regions corresponding to the region indicated by  $Z$  in Fig. 1. In addition, current could stay within the lumen beyond the outflow pipette tip and cross the epithelium in regions indicated by  $Y$  in Fig. 1. Therefore, the useful measure to compute the space constant is the ratio of

voltage deflection at the microelectrode to the voltage deflection at the input pipette. This ratio is given by:

$$\frac{V(x)}{V(0)} = \frac{\cosh\{(W/\lambda)[1 - (x/W)]\}}{\cosh(W/\lambda)}, \quad (6)$$

where  $V(0)$  is the voltage deflection at the input pipette.

Preliminary computations indicated that, even if the entire lateral cell surface allowed free conduction, the results would be very little different from the simplified case. The simplified case were therefore used for the treatment of all data. The data provide a check on whether the simplified case can be used. If the value of the space constant  $\lambda$  obtained from luminal punctures is the same as that derived from cellular punctures, then there is no measurable longitudinal current flow through the cells.

## Results

### The tissue space constant

Preliminary experiments showed that repeated punctures led to progressively lower resistance values, suggesting that the gut did not seal well after removal of the microelectrode. Hence, each tissue was impaled only once. It was impaled soon after cannulation, and the electrode was left then in place so that the voltage and voltage responses could be followed over time.

In later experiments, the voltage deflection at the outflow pipette was also measured. There were two criteria to be met for an acceptable reading of luminal voltage. The first was that all three readings, at the input perfusion pipette, at the outflow perfusion pipette and at the microelectrode, were all within 2 mV of one another whenever current was not passed. The second criterion was that the voltage deflection from the microelectrode should be smaller than that from the input pipette and greater than that from the outflow pipette. It became clear during these experiments that the voltage deflection from a cellular penetration was much lower than that from a luminal penetration, normally less than 20% of it. Hence, the criteria used for the early experiments were (i) identity of the perfusion pipette and microelectrode voltages at rest and (ii) that the microelectrode voltage deflection be at least 20% of that at the perfusion pipette. Twenty-one experiments fulfilled these criteria and were used for the determination of the space constant,  $\lambda$ .

### Physical measurements

The resistivity of the solution used both for perfusing and bathing the tissue was 43.1  $\Omega$  cm. The mean distance between the inflow and outflow pipettes ( $W$  in Fig. 1) was 733  $\pm$  41.9  $\mu$ m ( $N=21$ ). The distance beyond the outflow pipette and the tie ( $Y$  in Fig. 1) was estimated to average 367  $\mu$ m. The external diameter, as determined by optical measurements, was 287  $\pm$  5.1  $\mu$ m ( $N=22$ ). The tissues are usually translucent upon mounting, and it is possible obtain an estimate of cell height from the differences in light transmission. Height, measured this way, was approximately 45  $\mu$ m. Hence, luminal diameter

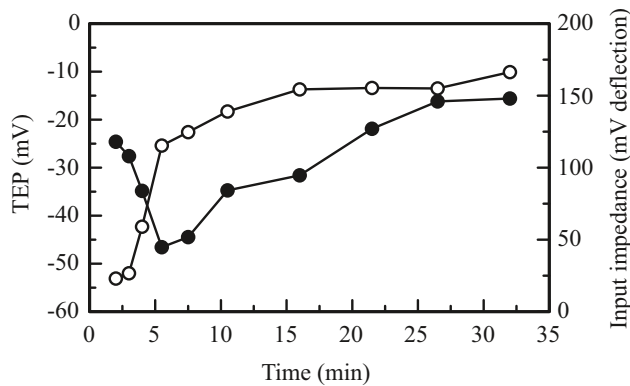


Fig. 2. Time course of the transepithelial voltage (TEP) (open circles, left-hand scale) and the input impedance as measured by input pipette deflection (filled circles, right-hand scale) in a typical experiment.

was estimated to be  $197\ \mu\text{m}$ . Microscopic analysis of fixed slides cut perpendicular to the long axis of the gut gave a value of cell height of  $63 \pm 0.68\ \mu\text{m}$  ( $N=166$ ). If this value is used, luminal diameter ( $a$ ) is computed to be  $162\ \mu\text{m}$ .

#### Changes in luminal voltage and resistance over time

As reported previously, the transepithelial potential (TEP) decays with time (Clark et al., 1999). There is an early phase during which TEP falls rapidly (becomes less negative). This ends after approximately 5 min and is followed by a second phase during which depolarization is much slower (see Fig. 2). When tissues were cannulated and perfused rapidly, the input impedance (as measured from the input perfusion pipette) of the gut followed a biphasic response. It was initially high and fell during the early period when the voltage was falling rapidly. Thereafter, it rose. Of the 21 experiments reported here, 14 provided readings within the first 5 min after cannulation. We detected the initial fall in nine of these. All tissues showed a subsequent rise in input impedance during the time that TEP was either falling slowly or constant. Since we do not know the total current in the region between the pipette tips (see above), we cannot convert the voltage deflection to a resistance. However, in any preparation, the fraction of the current that flowed out beyond the pipette tips, in the regions labeled  $Z$  and  $Y$  in Fig. 1A, would be expected to remain constant. Hence, changes in the voltage deflection seen at the input pipette reflect changes in the input impedance. We shall use the term 'input pipette impedance measure' for this voltage deflection. Fig. 2 shows the changes in potential and impedance in a typical experiment.

#### Estimate of the space constant

All measurements were taken between 23 and 28 min. The space constant,  $\lambda$ , was estimated in each experiment from the ratio of the voltage deflection of the microelectrode to the voltage deflection at the input perfusion pipette. Each experimental ratio gave a value of  $\lambda$  from equation 6. These values were then averaged to give a mean value of  $\lambda$  of

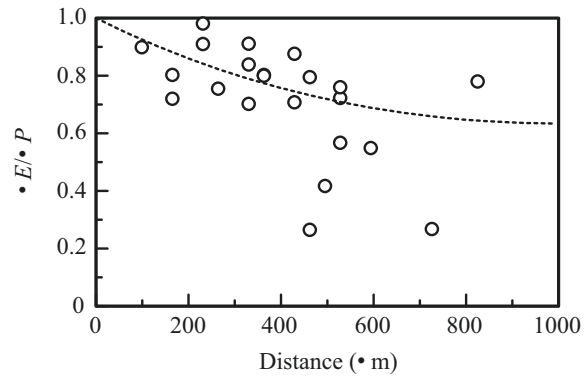


Fig. 3. Ratios of voltage deflection at the luminal pipette to voltage deflection at the input pipette as a function of distance from the input pipette.  $\Delta E/\Delta P$  is the ratio of voltage deflection at the microelectrode to voltage deflection at the input pipette. Each ratio implies a value of  $\lambda$  from equation 6. The dashed line is computed from  $\lambda=936\ \mu\text{m}$ , the average of the individual values of  $\lambda$ , where  $\lambda$  is the space constant of the tissue.

$936 \pm 84.5\ \mu\text{m}$  ( $N=21$ ). Fig. 3 depicts the values of the voltage deflection ratio as a function of distance from the input perfusion pipette. The curve is the voltage decrement computed from the mean value of  $\lambda$ . It should be noted that this is the mean of the space constants, not the mean of the individual points.

#### Cellular basal potentials

Two populations of cells were detected. One group had stable basal potentials, whereas in the second, the basal potential decayed along a time course similar to that of the TEP.

#### Cells in which the basal potential was stable

The usual criteria for an acceptable cell puncture were used; entry had to be sharp, the voltage had to remain stable for at least 1 min and had to return to within 2 mV of the baseline value upon removal. In addition, the voltage had to be different from the luminal voltage. One hundred successful impalements were recorded. All showed a basal resistance that was much lower than observed in the luminal puncture experiments. The mean

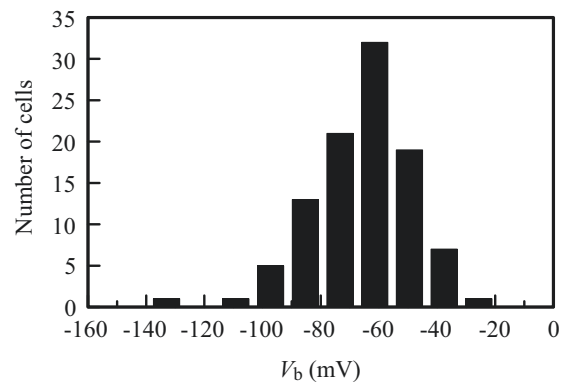


Fig. 4. Frequency distribution of basal voltages ( $V_b$ ) for the stable cell population.

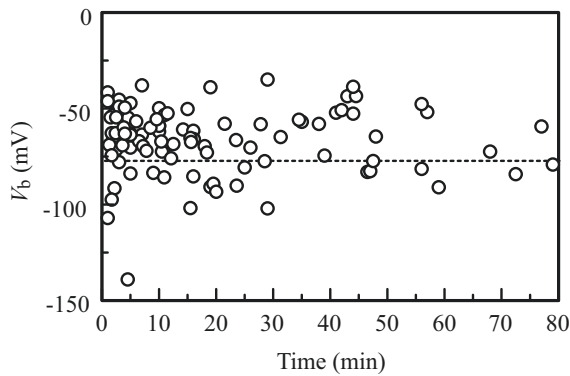


Fig. 5. Values of the basal voltage ( $V_b$ ) from the stable cells as a function of time after isolation. The dashed line is the mean basal voltage from the population.

value of the basal voltage ( $V_b$ ) was  $66.1 \pm 1.76$  mV ( $N=100$ ). With the exception of a single cell that had a stable potential of  $-139$  mV, all appeared to belong to a single population. Fig. 4 shows the distribution of basal voltages in this group of cells. Fig. 5 shows that these cells were stable not only for an individual puncture but that  $V_b$  stayed constant as the TEP decayed from its initial value of approximately  $-60$  mV to near zero. Fig. 6 shows that these cells were distributed throughout the gut with no apparent localization.

Basal voltage deflection, in response to an injected current (basal voltage divider), although uniformly low, varied slightly as a function of distance along the gut. Fig. 7 shows that this measure of basal resistance can be fitted adequately with a curve that is 7% of the luminal voltage decrement.

#### Cells in which the basal potential decayed

Criteria for an acceptable puncture of this population of cells included sharp entry and return of the voltage to within 2 mV of the value measured in the bath upon removal. The voltage at early times was required to be more negative than the simultaneously measured luminal voltage. Finally, the voltage deflection upon current injection was required to be less than 20% of the deflection at the input pipette. Fig. 8 illustrates the

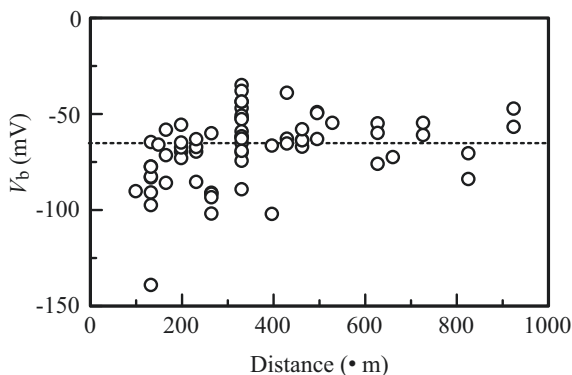


Fig. 6. Values of the basal voltage ( $V_b$ ) from the stable cell population as a function of distance from the input pipette. The dashed line is the mean basal voltage from the population.

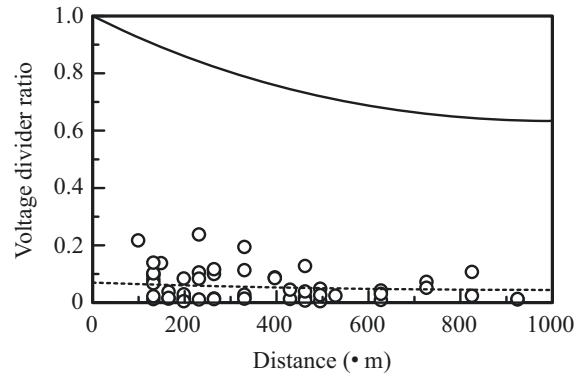


Fig. 7. Voltage divider ratio from the stable cell population as a function of distance from the input pipette. The solid line is the intraluminal voltage decrement using  $\lambda=936$   $\mu$ m, where  $\lambda$  is the space constant of the tissue. The dashed line is 0.07 times the intraluminal voltage ratio.

puncture of a decaying cell and compares the time course of this decay of  $V_b$  with that of the TEP. In Fig. 8, the voltage deflections from current injection in the input pipette recording have been removed to allow a better comparison of the two voltages. Fig. 8 also illustrates a frequent characteristic of the decaying cells; late in time,  $V_b$  is often less negative than is TEP.

Fig. 9 depicts the frequency distribution of the earliest values of  $V_b$  obtained in these decaying cells. All values were collected within 4 min of cannulation. The mean time after cannulation at which these voltages were collected was  $1.75 \pm 0.10$  min ( $N=45$ ). At that time, the mean basal membrane voltage was  $-100 \pm 3.2$  mV ( $N=45$ ) and the mean TEP was  $-38.8 \pm 3.3$  mV ( $N=45$ ). The high voltage values of this group are clearly characteristic of these cells. Because of the rapid changes in TEP and  $V_b$ , it is not clear whether the cluster exhibiting lower voltages (between  $-87$  and  $-55$  mV) are accurate measurements within a single voltage distribution, whether they represent a second population of decaying cells

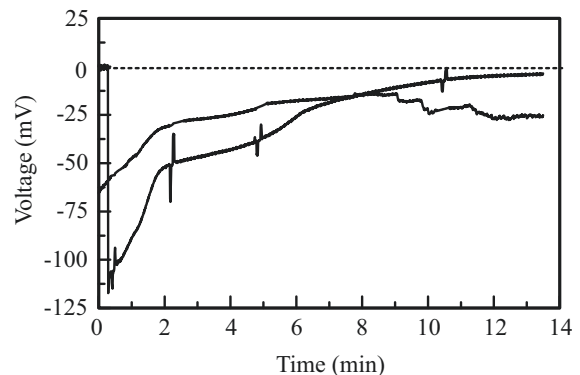


Fig. 8. Time course of transepithelial voltage and of basal voltage from a decaying cell as a function of time. The cell voltage recording shows the deflections from current injection. Deflections have been removed from the transepithelial voltage curve to allow the two to be distinguished. The dashed line is at zero potential.

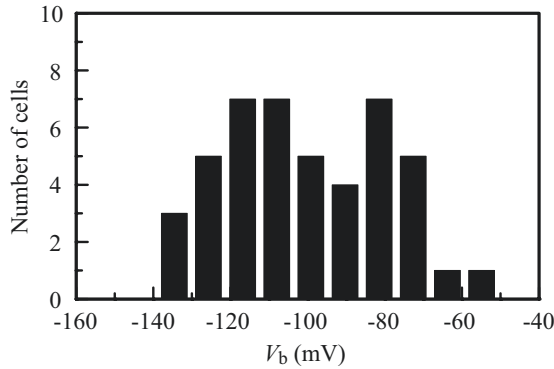


Fig. 9. Frequency distribution of basal voltages ( $V_b$ ) for the decaying cell population. All data were collected within 4 min of cannulation.

or whether they simply come from cells already showing significant decay. Other than their initial voltage, this group of lower-voltage decaying cells did not differ in any way from the group exhibiting higher initial voltages. The value of  $V_b$  given, of  $-100$  mV, is the mean of all the decaying cells. The decaying cells were distributed uniformly throughout the anterior stomach (Fig. 10).

At late times after cannulation,  $V_b$  of the decaying cells was characteristically slightly less negative to the hemolymph than was the lumen. Of the 19 punctures for which data at late times were obtained, 15 showed this phenomenon. The time of the late collections averaged  $15.35 \pm 1.68$  min, at which time TEP averaged  $-10.23 \pm 2.26$  mV and  $V_b$  averaged  $-9.28 \pm 2.03$  mV.

The basal voltage divider ratio was indistinguishable from that of the stable cells. It was uniformly low and decreased slightly with increasing distance along the gut. The same curve that described basal voltage deflection in the stable cells,  $7\%$  of  $\lambda$ , also described basal voltage deflection of this population (Fig. 11).

#### Effect of 5-HT

5-HT ( $10^{-4}$  mmol  $l^{-1}$ ) caused an immediate hyperpolarization in stable cells ( $N=13$ ). Prior to administration,  $V_b$  averaged

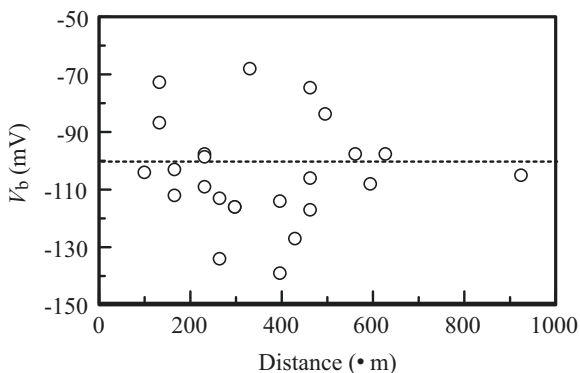


Fig. 10. Values of the basal voltage ( $V_b$ ) from the decaying cell population as a function of distance from the input pipette. The dashed line is the mean basal voltage from the population. All data were collected within 4 min of cannulation.

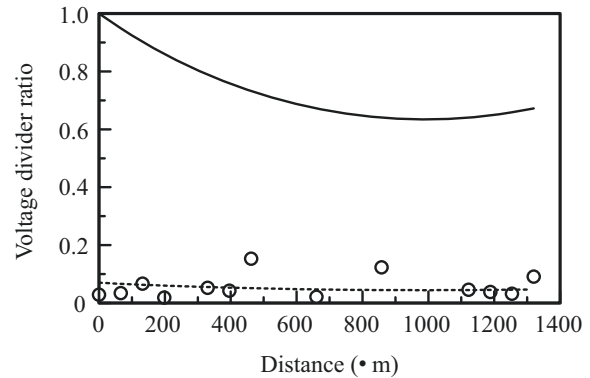


Fig. 11. Voltage divider ratio from the decaying cell population as a function of distance from the input pipette. The solid line is the intraluminal voltage decrement using  $\lambda=936$   $\mu$ m, where  $\lambda$  is the space constant of the tissue. The dashed line is 0.07 times the intraluminal voltage ratio. All data were collected within 4 min of cannulation.

$-83.0 \pm 6.8$  mV. Within 3 min of administration,  $V_b$  averaged  $-104 \pm 9.63$  mV, an average percentage change of  $24.4 \pm 2.9\%$ . These values are statistically different ( $P < 0.001$ ). At that time, there was no significant effect either on input pipette impedance measure (mean input impedance measure  $114 \pm 16.3$ ,  $N=11$ , before 5-HT and  $113 \pm 18.0$ ,  $N=11$ , after 5-HT) or on the voltage divider ratio (mean voltage divider ratio  $0.076 \pm 0.017$ ,  $N=10$ , before 5-HT and  $0.0809 \pm 0.024$ ,  $N=9$ , after 5-HT). There was a small increase in TEP; it increased from  $-4.95 \pm 1.06$  mV ( $N=12$ ) before to  $-8.04 \pm 2.07$  mV ( $N=12$ ) after 5-HT treatment. These values differ statistically ( $P < 0.001$ ). The full response of the cells to 5-HT was evident by 3 min; the mediator was washed off after 5 min. Interestingly, Clark et al. (1999) noted that the transepithelial hyperpolarization reached a maximum 15 min after application of the agent. Fig. 12 illustrates the response of

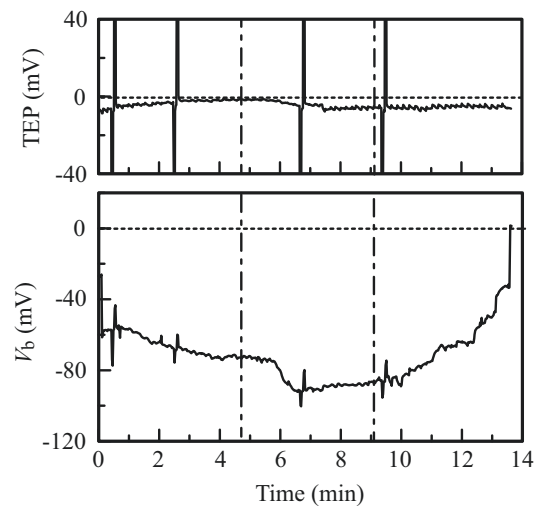


Fig. 12. Effects of 5-hydroxytryptamine (5-HT) on the basal potential of a stable cell. Upper curve, transepithelial potential (TEP). Lower curve, basal voltage ( $V_b$ ). The dashed lines in each figure are at zero potential. The left-hand vertical broken line indicates application of 5-HT. The mediator was rinsed off at the right-hand broken vertical line.

a stable cell to 5-HT. There was no change in input impedance or voltage divider ratio after 5-HT administration. 5-HT had no effect on  $V_b$  in decaying cells ( $N=9$ ), regardless of the time of application, although TEP increased in these cells as well.

### Discussion

The present work corroborates the previous work from this laboratory showing that the anterior stomach of the mosquito exhibits an inside-negative voltage that rapidly decays upon isolation. The previous publication also showed that administration of 5-HT produced a transepithelial hyperpolarization (Clark et al., 1999). The present work extends our understanding of the electrical properties of this epithelium and its cells.

#### *Validity of the results*

##### *The use of the simplified model*

Theoretical calculations of the complete model shown in Fig. 1A suggested that there was no reasonable possibility of appreciable longitudinal current between cells. The data collected here corroborate that statement. The finding that the voltage divider ratio was proportional to the space constant in all cells indicates that, in each cell, the same current density passed through the apical and basal membranes. This leads to the simplified model of Fig. 1B.

##### *Estimate of distance beyond the outflow pipette*

The value of  $Y$ , the distance beyond the outflow pipette and the tie, was crudely estimated to be approximately 370  $\mu\text{m}$ . No systematic study of this was made, but the value of  $Y$  was within 20% of that estimate in all cases. The value of  $Y$  does have an effect on that calculated space constant, but this level of uncertainty is trivial. A 20% error in the value of  $Y$  would have led to an error of only 3% in the computed value of  $\lambda$ .

##### *The decaying cells as a single separate population*

Cell impalements that decay are obviously suspect. We have two reasons to believe that these are accurate measurements of undamaged cells. First, they are seen only in the first few minutes after a tissue has been isolated. If the decay of  $V_b$  was because of damage, we would expect to damage cells later on in the experiment too. Second, the time course of the decay of  $V_b$  in these cells closely follows the time course of both the initial fall in input pipette impedance measure and the initial rapid fall in TEP. Since all the decaying cells had similar basal voltage divider ratios and a similar time course of decay, we believe that they were all samples from the same population and that the results were collected at slightly different times after isolation. Finally, the decaying cells did not respond to 5-HT, regardless of their initial  $V_b$ .

#### *The electrical parameters*

The space constant is  $9.36 \times 10^{-2}$  cm and  $\rho$  is 43.1  $\Omega\text{cm}$ . If we use the visual estimates of internal radius ( $a$ ) of 98  $\mu\text{m}$  and of cell height ( $b$ ) of 45  $\mu\text{m}$ , the estimate of the combined wall resistance  $r_m$ , as computed from  $\lambda^2 = ar_m/2\rho$ , is 73.8  $\Omega\text{cm}^2$ . If we

use the cell height from microscopic analysis of 63  $\mu\text{m}$ , then we compute an internal radius of 81  $\mu\text{m}$  and the estimate of  $r_m$  is 82.2  $\Omega\text{cm}^2$ . We regard these two estimates as in reasonably good agreement and will use the average values of  $a=93 \mu\text{m}$ ,  $b=53 \mu\text{m}$  and  $r_m=78 \Omega\text{cm}^2$  in subsequent calculations. We need to know the paracellular resistance  $r_p$  to calculate the apical and basal membrane resistances. We have no information on its value.

We shall make the calculation on the assumption that  $r_p = \infty$ . The error made this way is that the values that we calculate for  $r_a$  and  $r_b$ , the resistance of the tubule lumen and the cells, respectively, will be too low by an amount depending on the true value of  $r_p$ . The ratio of these values will, however, be accurate. Two equations describe the two unknowns,  $r_a$  and  $r_b$ . From equation 5, we have:  $78 = r_a + (93r_b/146)$ . From the voltage divider data, we obtain the relationship:  $(r_b/146)/(r_a/93) = 0.07$ . Simultaneous solution of these equations gives  $r_a = 72.9 \Omega\text{cm}^2$  and  $r_b = 8.0 \Omega\text{cm}^2$ .

These are the values at long times after isolation. Earlier in time, we believe that  $r_a$  is somewhat lower and that  $r_b$  is appreciably higher. It was not possible to obtain a satisfactory estimate of  $\lambda$  in the first minutes. This is probably because resistances were changing quite rapidly and at somewhat different rates in different preparations. However, since the input pipette impedance measure is nearly the same at very late times as it is upon cannulation, the value of  $\lambda$  would be similar at the two times.

Further studies of the transport physiology of the stomach would be greatly facilitated by an ability to voltage-clamp the tissue. The present study shows that acceptably uniform clamping could not be accomplished by injection of current through the perfusion pipette. Instead, an axial internal electrode will be required to achieve uniform current density throughout the length of the perfused gut.

##### *Is this a tight or leaky epithelium?*

A significant question for epithelial transport is whether this is a tight or a leaky tissue. There are at least three different ways of defining the degree of tightness. The first and simplest would be simply to compare  $r_m$  with that of other tissues. A second way, suggested by Guggino et al. (1982), would be to determine whether the resistance of the paracellular pathway is lower than that of the transcellular pathway. A low-resistance paracellular pathway is the defining characteristic of a leaky epithelium in this view. A third way would be to examine the ratio of  $\lambda$  to the length of the tubule. This measure defines whether a voltage change in one region of the tubule can have an effect in other regions. Again, a low ratio would define a leaky epithelium.

We shall use mammalian renal proximal tubule as an archetype for a leaky epithelium and mammalian renal distal tubule as an archetype for a tight epithelium. Typical values of  $r_m$  in renal proximal tubule are approximately 5  $\Omega\text{cm}^2$  and for renal distal tubule are 600  $\Omega\text{cm}^2$  (Boulpaep and Seely, 1971). In these terms, the mosquito anterior stomach appears to be intermediate.

We cannot directly apply the criterion suggested by Guggino

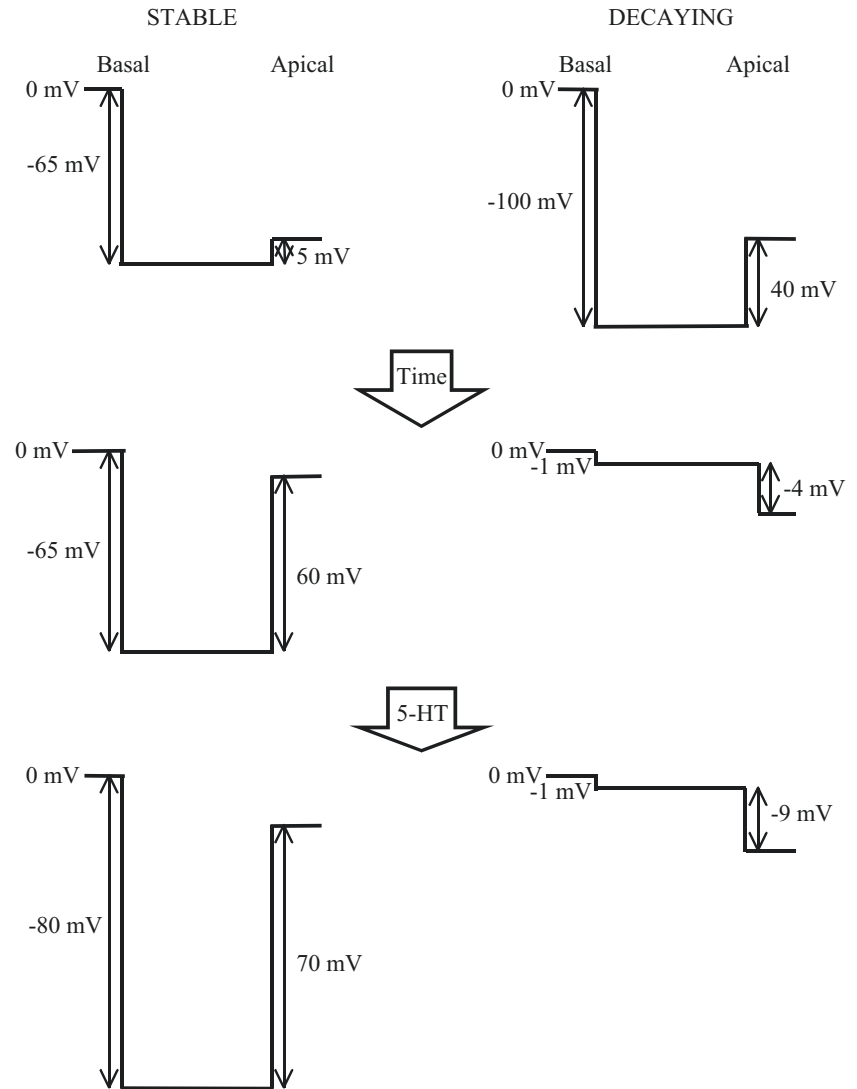


Fig. 13. Voltage profiles across stable cells (left side) and decaying cells (right side) upon isolation (top), 25 min after cannulation (middle) and after application of 5-hydroxytryptamine (5-HT) (bottom). The hemolymph side is on the left and the luminal side is on the right. All potentials are referred to the hemolymph bathing solution.

et al. (1992) since we did not measure the paracellular resistance. However, the data suggest that a significant fraction of the injected current did pass through the cells. In a similar study of ant Malpighian tubules, Leysens et al. (1992) did not detect any deflection in  $V_b$  upon current injection. They concluded that that tissue was a leaky epithelium. We did observe a deflection in  $V_b$  and, hence, current did pass through the cells. According to this criterion, we would decide that mosquito anterior stomach is probably a tight epithelium.

To use the third discriminator, we must know the length of the tubule *in vivo*. We shall estimate the lengths of the reference tubules from figures given for humans (1.4 cm for proximal convoluted tubule and 0.5 cm for distal convoluted tubule; Bloom and Fawcett, 1968) and divide by 2.6, a scaling factor derived from the relative glomerular filtration rates of human and dog kidney. The estimates of length so derived are 0.54 cm and 0.19 cm for canine proximal and distal convoluted tubules respectively. The space constant of canine proximal tubule is  $58 \mu\text{m}$ , and the ratio of space constant to length is  $58/5400=0.0108$ . The space constant of distal convoluted tubule is  $426 \mu\text{m}$ , and the ratio of space constant to length is

$426/1900=0.224$ . Both space constants were calculated from the data of Boulpaep and Seely (1971). These estimates are all somewhat imprecise but they might be expected to be approximately correct. The estimates of the ratio of  $\lambda$  to length differ by a factor of more than 20 between the two archetypal epithelial types. For the mosquito anterior stomach, the space constant is  $936 \mu\text{m}$  and the total length is approximately  $1600 \mu\text{m}$ . The ratio of  $\lambda$  to length is therefore  $936/1600=0.59$ . According to this criterion, the mosquito anterior stomach is clearly a tight epithelium. The finding that there was detectable current passing through the cells and the finding of a large ratio of space constant to organ length led us to conclude that this organ is a tight epithelium.

This conclusion seems consistent with what we know of the function of the anterior stomach. Although fat storage, presumably leading to fat absorption, has been observed (Wigglesworth, 1942), the only documented transepithelial movement is alkalization of the gut contents (Clements, 1992). A tight epithelium would seem necessary for the establishment and maintenance of the high pH gradient across the anterior stomach.

## Cell voltage profiles

The data allow us to construct voltage profiles of both types of cell and to look at how they change both over time and as a result of 5-HT application. Fig. 13 shows these profiles. Immediately after isolation, TEP is approximately  $-60$  mV. The decaying cells have a basal transmembrane potential  $V_b$  of  $-100$  mV and an apical transmembrane potential  $V_a$  of  $-40$  mV. Within 5 min,  $V_b$  collapses to a few millivolts and the potentials of the lumen, cell fluid and bathing solution are all within a few millivolts of each other. Later, TEP may be more negative than  $V_b$ . The stable cells start with a  $V_b$  of  $-65$  mV and a  $V_a$  of only  $-5$  mV. Soon (5 min) after isolation,  $V_a$  starts to rise so that, 25 min after isolation,  $V_b$  is still  $-65$  mV, but  $V_a$  is now  $-60$  mV. At that time, TEP is  $-5$  mV. The effect of 5-HT is to cause an immediate hyperpolarization of the basal membrane of the stable cells.

We do not have sufficient information to describe the processes that lead to these complex changes. We can, however, construct a scenario that is consistent with these changes. Upon isolation, the basal membranes of the decaying cell lose a trophic hormone. They immediately become very leaky. This accounts for the collapse of  $V_b$  in these cells, the collapse of TEP and the initial reduction of input impedance measure. Somewhat later, starting 4 or 5 min after isolation, the apical membranes of the stable cells become less conductive. Since there is no change in basal pump activity,  $V_b$  of these cells stays constant, but  $V_a$  rises. Since TEP is some sort of weighted average of the transepithelial voltage from both cell types, there is a further slow reduction in TEP, this time accompanied by a parallel increase in input impedance measure. This accounts for the second, slower phase of depolarization of TEP. The reversal of polarity of  $V_a$  in the decaying cells late in time is surely a peculiar finding. It could be a reflection of the reversal of net flux in an electrogenic antiport situated in the apical membrane. Finally, 5-HT enhances the activity of an electrogenic pump located in the basal membrane of the stable cells. Again, since TEP is an average of the activity of these two cell types, the response of  $V_b$  in the stable cells is more pronounced than is the response of TEP.

In summary, the present study shows that the anterior stomach of the mosquito midgut epithelium is a tight epithelial tissue. It contains two electrically distinct cell types. Changes in the properties of one cell type are associated with the decay of the transepithelial potential after isolation. Although, from a macroscopic viewpoint, 5-HT opposes the decline in transepithelial potential, its action is manifest in the stable cells rather than the decaying cells. This suggests that the 5-HT present in the hemolymph of the insect is not the sole factor that sustains the transport activities of the gut *in vivo*.

This research was supported by grants NRICGP 97-35302-4919 and NRICGP 99-35302-8371 to T.M.C. The authors would like to thank Mark Klowden and Gail DeSantis for eggs and Joan Folwell for preparation of the histological slides.

## References

- Bloom, M. and Fawcett, D. W.** (1968). *A Textbook of Histology*. Ninth edition. Philadelphia: W. B. Saunders.
- Boulpaep, E. L. and Sakin, H.** (1979). Equivalent electrical circuit analysis and rheogenic pumps in epithelia. *Fedn. Proc.* **38**, 2030–2036.
- Boulpaep, E. L. and Seely, J. F.** (1971). Electrophysiology of proximal and distal tubules in the autoperfused dog kidney. *Am. J. Physiol.* **221**, 1084–1096.
- Clark, T. M.** (1999). The evolution and adaptive significance of larval midgut alkalization in the insect superorder Mecoptera. *J. Chem. Ecol.* (in press).
- Clark, T. M. and Bradley, T. J.** (1997). Malpighian tubules of larval *Aedes aegypti* are hormonally stimulated by 5-hydroxytryptamine in response to increased salinity. *Arch. Insect Biochem. Physiol.* **34**, 123–141.
- Clark, T. M., Koch, A. and Moffett, D. F.** (1999). The anterior and posterior 'stomach' regions of larval *Aedes aegypti* midgut: regional specialization of ion transport and stimulation by 5-hydroxytryptamine. *J. Exp. Biol.* **202**, 247–252.
- Clements, A. N.** (1992). *The Biology of Mosquitoes*, vol. 1, *Development, Nutrition and Reproduction*, pp. 124–149. London: Chapman & Hall.
- Dadd, R. H.** (1975). Alkalinity within the midgut of mosquito larvae with alkaline-active digestive enzymes. *J. Insect Physiol.* **21**, 1847–1853.
- Dadd, R. H.** (1976). Loss of midgut alkalinity in chilled or narcotized mosquito larvae. *Ann. Ent. Soc. Am.* **69**, 248–254.
- Dow, J. A. T.** (1986). Insect midgut function. *Adv. Insect Physiol.* **19**, 187–328.
- Edwards, H. A.** (1982a). Ion concentration and activity in the haemolymph of *Aedes aegypti* larvae. *J. Exp. Biol.* **101**, 143–151.
- Edwards, H. A.** (1982b). Free amino acids as regulators of osmotic pressure in aquatic insect larvae. *J. Exp. Biol.* **101**, 153–160.
- Filippova, M., Ross, L. S. and Gill, S. S.** (1998). Cloning of the V-ATPase B subunit cDNA from *Culex quinquefasciatus* and expression of the B and C subunits in mosquitos. *Insect Mol. Biol.* **7**, 223–232.
- Gill, S. S., Chu, P. B., Smethurst, P., Pietrantonio, P. V. and Ross, L. S.** (1998). Isolation of the V-ATPase A and C subunit cDNAs from mosquito midgut and Malpighian tubules. *Arch. Insect Biochem. Physiol.* **37**, 80–90.
- Guggino, W. B., Windhager, E. E., Boulpaep, E. L. and Giebisch, G.** (1982). Cellular and paracellular resistances of the *Necturus* proximal tubule. *J. Membr. Biol.* **67**, 143–154.
- Hodgkin, A. L. and Rushton, W. A. H.** (1946). The electrical constants of a crustacean nerve fibre. *Proc. R. Soc. Lond. B* **133**, 444–479.
- Klein, U., Koch, A. and Moffett, D. F.** (1996). Ion transport in Lepidoptera. In *Biology of the Insect Midgut* (ed. M. J. Lehane and P. F. Billingsley), pp. 236–264. London: Chapman & Hall.
- Knowles, B. H.** (1994). Mechanism of action of *Bacillus thuringiensis* insecticidal  $\delta$ -endotoxin. *Adv. Insect Physiol.* **24**, 275–308.
- Leysens, A., Steele, P., Lohrmann, R. and Van Kerkhove, E.** (1992). Intrinsic regulation of  $K^+$  transport in Malpighian tubules (*Formica*): Electrophysiological evidence. *J. Insect Physiol.* **38**, 431–446.
- Wigglesworth, V. B.** (1942). The storage of protein, fat, glycogen and uric acid in the fat body and other tissues of mosquito larvae. *J. Exp. Biol.* **19**, 56–77.